

Valley symmetry breaking in bilayer graphene: a test to the minimal model

Masaaki Nakamura,¹ Eduardo V. Castro,^{2,3} and Balazs Dora⁴¹Department of Physics, Tokyo Institute of Technology, Tokyo 152-8551, Japan²Instituto de Ciencia de Materiales de Madrid, CSIC, Cantoblanco, E-28049 Madrid, Spain³Centro de Física do Porto, Rua do Campo Alegre 687, P-4169-007 Porto, Portugal⁴Max-Planck-Institut für Physik Komplexer Systeme, Nothnitzer Str. 38, 01187 Dresden, Germany
(Dated: February 22, 2024)

Physical properties reflecting valley asymmetry of Landau levels in a biased bilayer graphene under magnetic field are discussed. Within the 4-band continuum model with Hartree-corrected self-consistent gap and finite damping factor we predict the appearance of anomalous steps in quantized Hall conductivity due to the degeneracy lifting of Landau levels. Moreover, the valley symmetry breaking effect appears as a non-semiclassical de Haas-van Alphen effect where the reduction of the oscillation period to half cannot be accounted for through quasi-classical quantization of the orbits in reciprocal space, still valley degenerate.

PACS numbers: 73.43.Cd, 71.70.Dj, 81.05.Uw, 72.80.Le

Graphene, a two-dimensional hexagonal crystal of carbon atoms, has attracted enormous attention in recent years [1]. Its quasiparticles are massless Dirac fermions propagating with a velocity $v = 300$ of the speed of light. This allows us to discuss and even observe a variety of peculiar (ultrarelativistic) phenomena in a condensed matter system, such as the anomalous quantum Hall effect (QHE), the universal minimum conductivity, Klein tunneling, Zitterbewegung and Schwinger's pair production [2].

Departures from strict two-dimensionality promises interesting physics as well. A bilayer graphene (BLG), which consists of a pair of single graphene sheets bound by weak interlayer Van der Waals forces, has also been studied extensively [3, 4]. Its low energy excitations possess chiral symmetry and a quadratic spectrum, thus combining Dirac and Schrodinger like features. Moreover, BLG offers interesting opportunities regarding device applications. Breaking the layer symmetry opens an energy gap between valence and conduction bands which in addition can be tuned by electric field effect [5, 6, 7, 8] – a clear advantage compared to current technology semiconductors.

Establishing on a firm ground what is the minimal model describing the system is an important step towards real device applications. For instance, in the early experiments in BLG the gap was shown to be tunable between zero (gapless) and mid-infrared energies [5, 7], which has been confirmed very recently by infrared spectroscopy [9, 10]. The relevant minimal model has thus to correctly describe BLG up to mid-infrared energies, which is a stringent restriction to the available possibilities.

In the present paper we address the behavior of BLG in high magnetic and electric fields applied perpendicularly. Using as a minimal description the 4-band continuum model with Hartree-corrected self-consistent gap we predict new physics to take place at high enough fields. Specifically, for magnetic fields between 20–30 T and

electric fields between 0.5–1 V nm⁻¹ (i.e. densities $5–10 \times 10^{12}$ cm⁻² in the standard 300 nm SiO₂ back gate setup), both within experimental reach, we have found that a significant valley asymmetry is present with the following consequences: (i) the period of de Haas-van Alphen (dHvA) oscillations halves, in a clear non-semiclassical behavior; (ii) the QHE shows a new quantization rule for the Hall conductivity given by $\sigma_{xy} = 2\frac{e^2}{h}n$, with $n = 0; \pm 1; \pm 2; \pm 3; \dots$. Observing experimentally this new behavior would put on a firm ground our current understanding of BLG.

Model. We adopt the 4-band continuum model as a key ingredient in our minimal description. The Hamiltonian for one of the two valleys (K point) is given by the following 4 × 4 matrix [4, 6, 11] whose elements correspond to the A and B sublattices of the top and bottom layers (A₁; B₁; A₂; B₂),

$$H_K = \begin{pmatrix} 2 & v & 0 & t_2 \\ 6v & 0 & 0 & 7 \\ 4 & 0 & 0 & v \\ t_2 & 0 & v & 5 \end{pmatrix}; \quad (1)$$

where $v = \hbar^{-1}mv_F$ and the vector $\mathbf{p} + e\mathbf{A}$ is the momentum operator in a magnetic field $\mathbf{r} = (0; 0; B)$. The parameter $v_F \approx 10^6$ m s⁻¹ is the single layer Fermi velocity and $t_2 \approx 0.3$ eV the interlayer hopping energy [2]. Note that the zero entries in Eq. (1) can be filled with next-nearest-interlayer hoppings originating trigonal warping and electron-hole symmetry breaking effects [11]. At the energy scales we are interested in here, however, these terms can be neglected in a minimal description [4, 12]. The parameter t_2 accounts for the layer asymmetry induced by an external perpendicular electric field $\mathbf{E} = (0; 0; E_{\text{ext}})$. One way to relate t_2 and the applied electric field E_{ext} is by writing the local potential as a sum of two opposite contributions, one coming from the electrostatic energy due to E_{ext} which tries to polarize the system and a counteractive one originating

in the screening properties of the system. In the Hartree approximation can then be written as [6, 72]

$$2 = eE_{\text{ext}}c_0 + \frac{e^2c_0}{2\epsilon_0\epsilon_r} n; \quad (2)$$

where $c_0 \approx 3.4 \text{ \AA}$ is the interlayer distance, ϵ_0 is the permittivity of vacuum, ϵ_r is the relative permittivity of the system [13], and $n = n_{\text{top}} - n_{\text{bottom}}$ is the charge carrier imbalance between top and the bottom layers. A self-consistent procedure is then followed since n depends directly on the weight of the wave functions in each layer. Instead of E_{ext} we use the density n as an externally tunable parameter. The two are related as $E_{\text{ext}} = en/(2\epsilon_0\epsilon_r)$ in the standard back-gate configuration [14].

In zero magnetic field the system has a dispersion relation with the characteristic double-minimum structure [18]. In the presence of a finite magnetic field we can diagonalize the problem by going to the Landau level (LL) basis [19]. Using the Landau gauge $A = (-yB/2; 0, 0)$, and noting that the commutation relation between the momentum operators is $[p_x, p_y] = -2eB\hbar$, we define creation and annihilation operators of the harmonic oscillator as $p_x/\sqrt{2\hbar} = \sqrt{2eB}\hat{a}$ and $p_y/\sqrt{2\hbar} = \sqrt{2eB}\hat{a}^\dagger$ for $eB > 0$, where $\ell^2 = \hbar/(eB)$ is the magnetic length. Eigenvalues and eigenstates of Eq. (1) are then obtained by assuming the wave function to be a linear combination of the number states of the harmonic oscillator $|j\rangle$, with integer $j \geq 0$. The LLs, labeled by an integer $k \geq 0$, are given by

$$E_k = \frac{\hbar\omega_c}{2} \left(\frac{1}{2} + k \right); \quad (s_1; s_2); \quad (3)$$

with $r = \frac{1}{2} \frac{\hbar}{m^*v_F}$ and $d = \frac{1}{2} \frac{\hbar}{m^*v_F}$. The label $(s_1; s_2)$ specifies the outer and the inner bands ($s_1 = \pm 1$) and positive and negative ($s_2 = \pm 1$) energies, respectively. For $k \geq 2$ the parameter is given by the roots of the fourth-order polynomial

$$(2k^4 - 1 + \ell^2 + 2d^2)k^2 - 2d^2 + [k(k-1) + d^2(d^2 + r^2 - 2k + 1)] = 0; \quad (4)$$

and the Landau states are

$$|k; ii\rangle = \frac{1}{\sqrt{k!}} \left(\frac{r}{\ell} \right)^k |k-1; i\rangle + \frac{1}{\sqrt{k!}} \left(\frac{r}{\ell} \right)^k |k-2; i\rangle + \frac{1}{\sqrt{k!}} \left(\frac{r}{\ell} \right)^k |k-1; i\rangle; \quad (5)$$

where the coefficients are given by $c_k = \frac{r}{\ell} \frac{1}{k!} \frac{1}{(k+1)!}$, $c_k = \frac{r}{\ell} \frac{1}{k!} \frac{1}{(k+1)!}$ and the normalization condition. In addition there are the LLs $k = 1$ and $k = 0$. In the former case is given by the roots of

$$3d^2 + (d^2 + r^2)(d^2) = 0; \quad (6)$$

and the Landau state can be expressed as

$$|1; ii\rangle = \frac{1}{\sqrt{2}} |1; i\rangle + \frac{1}{\sqrt{2}} |1; i\rangle; \quad (7)$$

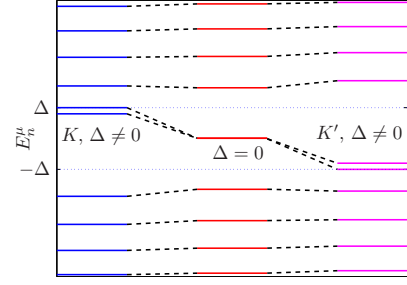


FIG. 1: (color online). A symmetric structure of Landau levels at K and K' points in bilayer graphene with energy difference Δ .

Note that Eq. (6) has only three roots, while provides four labellings. We reserve the label $(-; +)$ for the $k = 0$ LL, where $= +d$ provides the only eigenvalue. We then write the respective Landau state as $|j; -; +\rangle$

$|0; j; 0; 0\rangle^T$. The two states $|j; -; +\rangle$ and $|j; -; +\rangle$ are degenerate in the gapless case $d = 0$ [4]. For the K' point the Hamiltonian is given by Eq. (1) with the replacement $\ell \rightarrow -\ell$. Note that Eqs. (4) and (6), which determine the eigenvalues, include a linear term in d so that LLs for K and K' points are not identical for $d \neq 0$ (see Fig. 1). The eigenvalues and eigenstates are then obtained by replacing $d \rightarrow -d$ in Eqs. (4) and (6) and by reversing the order of the elements in vectors (5) and (7). As for the $k = 0$ LL at K' we reserve the label $(-; -)$ since the respective eigenvalue has $= -d$, and write the eigenstate as $|j; -; -\rangle = |0; 0; j; 0\rangle^T$.

The final ingredient in the present model is the LL broadening. This is taken into account through a constant imaginary retarded self-energy $\text{ret} = i$. Regarding the relevant value of ω we note that the dominant source of scattering originates from ripples and charged impurities [20]. Since BLG is less rippled than its monolayer counterpart, and charged impurities do not penetrate in between the layers, they mainly affect the layer closer to the substrate, we take $\omega \approx 0.01t_F$ as a conservative estimate. This phenomenological value is to be expected for a system ballistic on the submicrometer scale and, moreover, when used to get the longitudinal resistivity (by inverting the conductivity tensor given below) it compares well with experiments in Ref. [3].

Self-consistent gap. The gap defined in Eq. (2) is obtained by writing the charge imbalance n in terms of the LL weight in different layers,

$$n = \frac{1}{\ell^2} \sum_{k=0}^{\infty} \left(f(E_k) \left(\frac{r}{\ell} \right)^2 + \left(\frac{r}{\ell} \right)^2 \left(\frac{r}{\ell} \right)^2 \left(\frac{r}{\ell} \right)^2 \right) \quad (8)$$

where the first and the second terms denote contributions

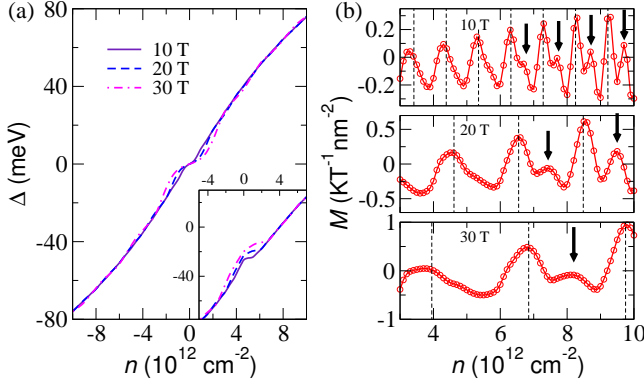


FIG. 2: (color online). (a) Δ vs n for different values of magnetic field. The inset shows the case of a fixed top-gate. (b) Magnetization vs n for different values of magnetic field. The vertical lines signal the semiclassical period.

from K and K^0 points, respectively. The factor $1/(l^2)$ is the degeneracy of LLs per system volume. The function $f(E)$ is the Fermi distribution function in the presence of LL broadening,

$$f(x) = \frac{1}{2} \left[1 - \tan^{-1} \frac{x}{(x^2 + l^2)^{1/2}} \right] (k_B T)^{-1}; \quad (9)$$

valid in the low temperature limit $k_B T \ll \Delta$. In Eq. (9) the chemical potential is given by

$$n = \frac{1}{l^2} \sum_{k=0}^{\infty} \int_{-\infty}^{\infty} f(E_k) dE_k \quad (10)$$

for a given density n , where $f(x) = f(x) - f(x + \Delta)$. The solution is obtained numerically by solving Eqs. (2) to (10) till self-consistency is achieved [16].

In Fig. 2(a) we show the self-consistent asymmetry gap at $T = 0$ as a function of electron density n . Increasing the applied magnetic field increases screening around $n = 0$, which can be traced back to the valley (layer) asymmetry of the 0th and 1st LLs [see Eq. (7)]. In particular, the 0th LL appears fully polarized (layer 1 at K and layer 2 at K^0) thus giving the dominant contribution to screening whenever the Fermi level lies in between the two. The inset shows the case of a finite top-gate voltage fixed at $n_{tg} = 2 \times 10^{12} \text{ cm}^{-2}$ [14]. The case of fixed filling factor and varying magnetic field was considered in Ref. [17] without LL broadening.

dHvA effect. As a consequence of LL quantization the magnetization due to the orbital motion of electrons shows periodic oscillations as a function of inverse magnetic field (dHvA effect). Equivalently, in systems where the carrier density can be tuned, similar oscillations show up as Δ changes. Here we address the dHvA effect in BLG at fixed magnetic field B and varying n through a back-

gate voltage, taking into account that E_{ext} changes as the back-gate voltage is tuned.

The magnetization for fixed density n is given as $M = \partial(B; (n))/\partial B$, where Φ is the Gibbs free energy and (n) is the chemical potential satisfying Eq. (10) [21]. The Gibbs free energy in the presence of LL broadening is obtained after standard treatment and is given by

$$\Phi(B; n) = \frac{V}{4\pi^2 l^2} \sum_{k=0}^{\infty} \int_{-\infty}^{\infty} dE e^{-\beta E} f(E) g(E - E_k + \Delta); \quad (11)$$

where $f(x) = (e^x + 1)^{-1}$ is the Fermi distribution function with $\beta = 1/(k_B T)$ and $g(x) = 2 \tan^{-1}(x/l)$, the volume (area) of the system is V , and l includes not only the band indices (s_1, s_2) but also the valley index. With the experimental conditions $k_B T$ in mind we consider the $T = 0$ version of Eq. (11), which still has to be evaluated numerically along with the magnetization. In particular, summation over the LLs is performed by introducing a finite LL cutoff k_c . We choose discrete values of the magnetic field B so that the number of states taken into account to obtain n is preserved. Since $k > 1$ LLs have the same degeneracy proportional to the magnetic field, and since the degeneracy of $k = 0$ and $k = 1$ LLs add up to the same value, it is enough to choose the magnetic field B_{k_c} discrete values as $k_c B_{k_c} = \text{Const}$ [22]. A similar idea has been used for monolayer graphene in Ref. [23].

In Fig. 2(b) we show the dHvA effect as the carrier density is changed at magnetic fields $B = 10; 20; 30 \text{ T}$. The vertical dashed lines signal the oscillation period given by the semiclassical approach. The latter applied to a two-dimensional system in constant magnetic field and varying density implies: a peak in magnetization whenever the semiclassical orbit coincides with the Fermi surface; a complete oscillation whenever the area enclosed by the Fermi surface A changes by the quantum of area enclosed by the semiclassical orbit, $\Delta A = eB = h$ [24, 25]. Owing to the cylindrical symmetry of the bands [Eq. (1)] the oscillation period can be expressed in terms of carrier density as

$$n = 2 \frac{eB}{h}; \quad (12)$$

where we used $A = \pi r^2$ and included spin and valley degeneracies. When n (i.e. the gap) is small the oscillations in magnetization follow the semiclassical prediction [Fig. 2(b)]. With increasing n (i.e. larger gap) we observe deviations from the semiclassical value [arrows in Fig. 2(b)] and the new oscillation period is half of Eq. (12). This provides a clear sign of the valley symmetry breaking, whose experimental observation could be possible by diamagnetic current measurements. Moreover, oscillations with a period which is half of Eq. (12) should also be observed in longitudinal conductivity (Shubnikov-de Haas oscillations).

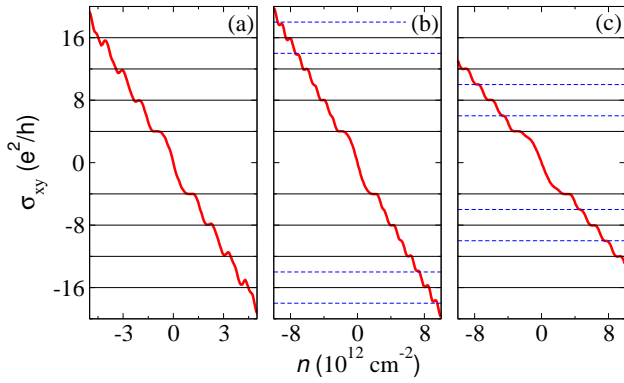


FIG. 3: (color online). Hall conductivity vs electron density at different magnetic fields: $B = 10$ T (a), 20 T (b), 30 T (c).

QHE. The QHE is discussed by extending the results of Ref. [26] for the gapless BLG case. We use the Kubo formula to get the longitudinal and Hall conductivities,

$$\text{Re } \sigma_{ij}(\omega) = \frac{\text{Im } \tilde{\chi}_{ij}(\omega + i)}{\omega}; \quad (13)$$

where $\tilde{\chi}_{ij}(\omega) = \chi_{ij}(\omega) - \chi_{ij}(0)$ with $\chi_{ij} = 2 \text{fx}; \text{yg}$. The polarization function $\chi_{ij}(\omega)$ is given by the current-current correlation function, and obtained as the analytical continuation of the Matsubara form :

$$\tilde{\chi}_{ij}(\omega) = \frac{e^2}{2} \frac{\sum_{n=1}^{\infty} \sum_{k,l} \chi_{ij}(k; j_l) \chi_{ij}(l; i_k)}{(\omega_n^2 - \omega^2)(\omega_n^2 - \omega^2)}; \quad (14)$$

where χ_{ij} and ω_n include not only the band indices but also the valley index. The matrix χ_{ij} is defined by $\chi_{ij} = r_{ij} H$, and $\omega_n^2 = E_k^2 - E_k^2$ with LL E_k as in Eq. (3). We have defined $\omega_n^2 = \omega_n^2 + [+ \text{sgn}(\omega_n)] \omega$ and $\omega_n^2 = \omega_n^2 + \omega_m^2$ with ω_n (ω_m) as the Matsubara frequency of fermions (bosons).

Numerical results for the Hall conductivity as a function of carrier density (no top gate is assumed) are shown in Fig. 3 for different magnetic fields [27]. For $B = 10$ T the Hall conductivity follows the gapless BLG quantization rule $\sigma_{xy} = 4ne^2/h$ with $n = 1; 2; 3 \dots$. For $B = 20 - 30$ T new quantized Hall steps [dashed horizontal lines in Figs. 3(b) and 3(c)] appear at high carrier densities (large asymmetry gap). The new quantization rule reads $\sigma_{xy} = 2ne^2/h$ and is a direct consequence of the degeneracy lifting between LLs from K and K^0 . Including a top gate enables the observation of the new quantization rule near and at the neutrality point [15].

Conclusion. A remarkable property of BLG is the possibility to open and tune an energy gap by breaking the layer symmetry. At finite magnetic fields this layer asymmetry translates into an asymmetry between the two valleys, no longer protected by time-reversal symmetry. Using the 4-bands continuum model with

self-consistent gap and Landau-level broadening we have shown that the effects of valley symmetry breaking are manifested in non-semiclassical oscillations of the magnetization and anomalous quantized Hall steps. Their experimental detection is within reach, and would allow for a critical test of the minimal model for BLG.

We thank M. Koshino and M. A. H. Vozmediano for illuminating discussions. MN is supported by Global Center of Excellence Program "Nanoscience and Quantum Physics". EVC is financially supported by the Juan de la Cierva Program (MCI, Spain). BD was supported by the Hungarian Scientific Research Fund under grant number K 72613 and by the Bolyai program of the Hungarian Academy of Sciences. MN and EVC acknowledge the visitors program at the Max-Planck-Institut für Physik komplexer Systeme, Dresden, Germany.

-
- [1] A. K. Geim, Science 324, 1530 (2009).
 - [2] A. H. Castro Neto et al, Rev. Mod. Phys. 81, 109 (2009).
 - [3] K. S. Novoselov et al, Nat. Phys. 2, 177 (2006).
 - [4] E. M. C. Cann and V. I. Fal'ko, Phys. Rev. Lett. 96, 086805 (2006).
 - [5] T. Ohta et. al, Science 313, 951 (2006).
 - [6] E. M. C. Cann, Phys. Rev. B 74, 161403 (2006).
 - [7] E. V. Castro et al, Phys. Rev. Lett. 99, 216802 (2007).
 - [8] J. B. Oostinga et al, Nature Mat. 7, 151 (2007).
 - [9] Y. Zhang et al, Nature 459, 820 (2009).
 - [10] K. F. Mak et al, Phys. Rev. Lett. 102, 256405 (2009).
 - [11] J. Nilsson et al, Phys. Rev. B 78, 045405 (2008).
 - [12] E. V. Castro et al, arXiv:0807.3348.
 - [13] The value of ϵ_r depends on the substrate. For a SiO_2/air interface $\epsilon_r = 2.5$. Here we use $\epsilon_r = 1$ as a reference.
 - [14] In dual-gate cases E_{ext} and n are independent: $E_{\text{ext}} = e(n_{\text{bg}} - n_{\text{tg}}) = (2\epsilon_0 \epsilon_r)$ and $n = n_{\text{bg}} + n_{\text{tg}}$, where n_{bg} and n_{tg} are back- and top-gate induced densities [8, 15].
 - [15] S. Kim and E. Tutuc, arXiv:0909.2288.
 - [16] The LL sum in Eqs. (8) and (10) is cut off at $k_c = 1000$. A similar approach was followed in Ref. [17].
 - [17] M. Mucha-Kruczynski, E. M. C. Cann, V. I. Fal'ko, Solid State Commun. 149, 1111 (2009).
 - [18] F. Guinea, A. H. Castro Neto, N. M. R. Peres, Phys. Rev. B 73, 245426 (2006).
 - [19] J. M. Pereira, Jr., F. M. Peeters, and P. Vasilopoulos, Phys. Rev. B 76, 115419 (2007).
 - [20] M. I. Katsnelson and A. K. Geim, Phil. Trans. R. Soc. A 366, 196 (2008).
 - [21] S. G. Sharapov, V. P. Gusynin, and H. Beck, Phys. Rev. B 69, 075104 (2004).
 - [22] We use $k_c = 1000$ and checked consistency of results.
 - [23] M. Koshino and T. Ando, Phys. Rev. B 75, 235333 (2007).
 - [24] L. Onsager, Philos. Mag. 43, 1006 (1952).
 - [25] I. M. Lifshitz and A. M. Kosevich, Zh. Eksp. Teor. Fiz. 29, 730 (1955).
 - [26] M. Nakamura, L. Hirasawa, and K. Imura, Phys. Rev. B 78, 033403 (2008).
 - [27] Summing over 100 LLs is enough for the conductivity.